

RESEARCH ARTICLE

Pericellular heparan sulfate proteoglycans: Role in regulating the biosynthetic response of nucleus pulposus cells to osmotic loading

Carly M. Krull¹ | Jordan Rife¹ | Brett Klamer² | Devina Purmessur^{1,3,4} | Benjamin A. Walter^{1,3,4} 

¹Department of Biomedical Engineering, The Ohio State University, Columbus, Ohio, USA

²Department of Biomedical Informatics, Center for Biostatistics, The Ohio State University, Columbus, Ohio, USA

³Department of Orthopedics, The Ohio State University Wexner Medical Center, Columbus, Ohio, USA

⁴Spine Research Institute, The Ohio State University, Columbus, Ohio, USA

Correspondence

Benjamin A. Walter, Department of Biomedical Engineering, The Ohio State University, Mars G. Fontana, 140 W. 19th Ave, Room 2124, Columbus, OH 43210, USA.
Email: walter.367@osu.edu

Funding information

National Center for Advancing Translational Sciences of the National Institutes of Health, Grant/Award Number: UL1TR002733; National Institute of Arthritis and Musculoskeletal and Skin Diseases, Grant/Award Number: R21AR076611; Ohio State University, Department of Biomedical Engineering

Abstract

Background: Daily physiologic loading causes fluctuations in hydration of the intervertebral disc (IVD); thus, the embedded cells experience cyclic alterations to their osmotic environment. These osmotic fluctuations have been described as a mechanism linking mechanics and biology, and have previously been shown to promote biosynthesis in chondrocytes. However, this phenomenon has yet to be fully interrogated in the IVD. Additionally, the specialized extracellular matrix surrounding the cells, the pericellular matrix (PCM), transduces the biophysical signals that cells ultimately experience. While it is known that the PCM is altered in disc degeneration, whether it disrupts normal osmotic mechanotransduction has yet to be determined. Thus, our objectives were to assess: (1) whether dynamic osmotic conditions stimulate biosynthesis in nucleus pulposus cells, and (2) whether pericellular heparan sulfate proteoglycans (HSPGs) modulate the biosynthetic response to osmotic loading.

Methods: Bovine nucleus pulposus cells isolated with retained PCM were encapsulated in 1.5% alginate beads and treated with or without heparinase III, an enzyme that degrades the pericellular HSPGs. Beads were subjected to 1 h of daily iso-osmotic, hyper-osmotic, or hypo-osmotic loading for 1, 2, or 4 weeks. At each timepoint the total amount of extracellular and pericellular sGAG/DNA were quantified. Additionally, whether osmotic loading triggered alterations to HSPG sulfation was assessed via immunohistochemistry for the heparan sulfate 6-O-sulfotransferase 1 (HS6ST1) enzyme.

Results: Osmotic loading significantly influenced sGAG/DNA accumulation with a hyper-osmotic change promoting the greatest sGAG/DNA accumulation in the pericellular region compared with iso-osmotic conditions. Heparinase-III treatment significantly reduced extracellular sGAG/DNA but pericellular sGAG was not affected. HS6ST1 expression was not affected by osmotic loading.

Conclusion: Results suggest that hyper-osmotic loading promotes matrix synthesis and that modifications to HSPGs directly influence the metabolic responses of cells to osmotic fluctuations. Collectively, results suggest degeneration-associated

This is an open access article under the terms of the [Creative Commons Attribution-NonCommercial](https://creativecommons.org/licenses/by-nc/4.0/) License, which permits use, distribution and reproduction in any medium, provided the original work is properly cited and is not used for commercial purposes.

© 2022 The Authors. *JOR Spine* published by Wiley Periodicals LLC on behalf of Orthopaedic Research Society.

modifications to pericellular HSPGs may contribute to the altered mechanobiology observed in disease.

KEYWORDS

heparan sulfate proteoglycan, intervertebral disc, mechanotransduction, nucleus pulposus, osmotic, pericellular matrix

1 | INTRODUCTION

The intervertebral disc (IVD) is the joint between vertebrae within the spine that facilitates motion while supporting physiologic loads. The IVD's ability to resist compressive forces arises predominately from osmotic swelling pressures, which develop due to the high concentration of proteoglycans within the tissue. The proteoglycans carry negative charges and impart the tissue a fixed charge density (FCD) which, as described by multiple theoretical frameworks,¹⁻⁴ interact with mobile ions and engender an osmotic swelling pressure. Thus, both the proteoglycan content and ionic concentration together establish the IVD's osmotic environment. This classic structure–function relationship influences mechanical behaviors of the IVD, and in turn, serves as a mechanobiological mechanism coupling mechanical loading and cellular biology.⁵⁻⁷

The IVD's mechanical behavior is associated with characteristic diurnal changes in tissue height and volume. During the daytime, as the tissue compresses and water is expelled, the disc loses ~20% of its volume, with complete recovery overnight.^{7,8} Accordingly, this daily change in disc volume and water content causes a cyclic fluctuation in FCD and corresponding intra-tissue osmolarity. Dynamic loading of the IVD, as compared with static loading, is recognized as essential for the maintenance of normal tissue biosynthesis and metabolism.^{9,10} This suggests that dynamic osmotic stimuli themselves may be similarly important in regulating cellular metabolism. Many studies have demonstrated that IVD cellular metabolism is sensitive to the osmotic environment, evidenced through alterations in gene, protein and ion channel expression,¹¹⁻¹⁴ cytoskeletal organization,¹⁵ as well as matrix production.^{5,16,17} In articular chondrocytes, load-induced changes in osmolarity elicit stronger anabolic cellular responses compared with static conditions and influence the activation of various ion channels.⁶ These findings further demonstrate dynamic osmotic environments are an important mechanobiologic stimuli. However, the specific contributions of osmotic fluctuations to the metabolic regulation of IVD cells remain unclear.

An extension of this classic structure–function relationship relating tissue composition to its osmotic swelling pressure emphasizes that spatial variations in the proteoglycan content must engender spatial variations in the osmotic environment. In particular, cells within the central nucleus pulposus (NP) region of the IVD are situated within regions of specialized extracellular matrix, often called a chondron, that differs from the extracellular matrix of the general tissue.¹⁸ The composition of a chondron varies spatially as it moves

towards the cell surface, with the area farther from the cell called the territorial matrix and transitioning to a thin layer of specialized extracellular matrix molecules, called the pericellular matrix (PCM) immediately adjacent to the cell surface. These territorial and pericellular regions are present within various orthopedic tissues and help transduce tissue-level loads to cells embedded within.^{19,20} To facilitate this transduction, the composition differs from the surrounding tissue. Specifically, the PCM region contains elevated levels of collagen VI and perlecan, a heparan-sulfated proteoglycan (HSPG).^{18,21,22} Perlecan, in particular, influences the biosynthetic response to osmotic loading through both mechanical and biological avenues. Mechanically, PCM FCD governs cellular volume changes during osmotic cycles, acting as both a physical barrier to swelling and an osmotic buffer situated directly at the cell surface.^{23,24} Biologically, HSPGs regulate cell phenotype in a variety of tissues, through interactions with growth factors as well as alterations in sulfation patterns associated with age and disease.²⁵ Collectively, these studies pinpoint HSPGs within the PCM as mediators of osmotic mechanotransduction and regulators of multiple biologic processes within the IVD.

Therefore, the objectives of this study were to determine: (1) whether dynamic osmotic conditions regulate biosynthetic activity in NP cells and (2) whether pericellular HSPGs modulate the biosynthetic response to osmotic loading. Our experiments test the hypotheses that: (1) dynamic osmotic conditions enhance proteoglycan synthesis and (2) HSPGs within the PCM directly regulate the biosynthetic response to osmotic loading. To investigate these hypotheses, cells were isolated with retained PCM, and heparinase III enzyme was used to selectively degrade the native HSPGs. Cells encapsulated in alginate were osmotically loaded for 1 to 4 weeks, with sulfated glycosaminoglycan (sGAG) accumulation and HSPG sulfation measured at each timepoint.

2 | METHODS

2.1 | Cell dissection, isolation, and encapsulation

Bovine caudal IVD tissue was obtained from a local abattoir within 8 h of death. An initial dose study identified the appropriate concentration of heparinase III for HSPG degradation. For these experiments, NP tissue was extracted from five discs originating from two bovine tails, with tissue pooled by tail. Then, for osmotic loading experiments, a separate cell isolation was performed for each time point (1, 2, or 4 weeks). Specifically, the first five levels of five bovine tails were

extracted, allotting a total of 25 IVDs per time point. At each isolation, tissue was pooled to provide sufficient cell number for experiments. Nucleus pulposus tissue was extracted, washed with 3% penicillin/streptomycin and 1.5% amphotericin B in $1\times$ PBS for 5 min, then minced, and placed into tubes. Cells were isolated enzymatically to retain the PCM, as previously described.²⁶ Briefly, digestion media (630 U/ml collagenase II, 1.5 U/ml dispase, 1% penicillin/streptomycin, and 0.5% amphotericin B in high glucose DMEM) was distributed to tubes of tissue at a ratio of 10 ml/g tissue.²⁷ Tissue incubated for 5 h at 37 °C with continuous agitation. After 5 h, the contents of each tube was strained through a 40–100 μ m mesh, and washed with DMEM. Isolated cells were counted via hemacytometer and suspended at 2×10^6 cells/ml in 1.5% alginate (Pronova UP LVG; NovaMatrix; Sandvika, Norway) in 0.15 M NaCl. To form alginate beads, the cell suspension was drawn into a 21-gauge needle, then added drop-wise to 102 mM CaCl_2 . Beads were placed on an orbital shaker for 10 min, then were washed three times: twice in 0.15 M NaCl to remove excess calcium, and a third time in DMEM adjusted to 400 mOsm/kg H_2O to remove excess ions.

2.2 | Degradation of HSPGs using heparinase III

Prior to osmotic loading experiments, a dose response study was conducted to determine an appropriate heparinase III dose for pericellular HSPG degradation. One day after cells were encapsulated within alginate beads they were treated with 0, 0.01, 0.1, and 0.5 U/ml heparinase III (H8891; Sigma; St. Louis, MO) for 4 h in culture media (10% FBS, 2% penicillin/streptomycin, 1% amphotericin B, and 0.2% 25 mg/ml ascorbic acid in high glucose DMEM adjusted to 400 mOsm/kg H_2O). After the treatment period, beads were rinsed and measured for cell viability and cell-associated (i.e., pericellular) sGAG/DNA content as described below. Additional beads were fixed in 10% neutral buffered formalin and used to assess heparin sulfate neopeptide (3G10) formation—a byproduct of heparin sulfate degradation or stained with toluidine blue as previously described²⁸ to qualitatively assess the pericellular matrix region.

2.3 | Application of osmotic loading

For osmotic loading experiments, half of beads received heparinase III at 0.1 U/ml 2 days prior to beginning of osmotic loading. A previously developed osmotic loading regime,⁶ consisting of placing beads in an altered osmotic environment for 1 h a day was used and beads were cultured for 1, 2, or 4 weeks. Specifically, alginate beads were cultured in media osmotically adjusted to 400 mOsm/kg H_2O for 23 h/day, then moved to one of three osmotically adjusted solutions for 1 h/day: static control (400 mOsm/kg H_2O), hyperosmotic (600 mOsm/kg H_2O), or hypo-osmotic (200 mOsm/kg H_2O). Media consisted of high glucose DMEM containing 10% FBS, 1% penicillin streptomycin, and 0.5% amphotericin B, with 0.2% 25 mg/ml ascorbic acid. Media osmolality was adjusted to within ± 2 mOsm/kg H_2O of the desired

osmolality using a freezing point osmometer (Model 3250, Advanced Instrument, Norwood, MA) by the addition of distilled water and sucrose. All media used for 1 h loading (400 static control, 600, and 200 mOsm/kg H_2O) was diluted equivalently to maintain constant nutrient availability between conditions. However, to ensure adequate nutrient availability for cell metabolism and biosynthesis, media used for 23 h culture was adjusted with 5 M sucrose, with the added volume accounting for <5% total media volume. Beads were cultured in custom 3D printed transwells and cultured at 37 °C, 5% CO_2 and 21% O_2 . Transwells facilitated easy transfer of beads between culture conditions, and were 3D printed from polycarbonate, with ~ 1 mm diameter holes at the base for media perfusion (Figure S1).

2.4 | Cell viability and sulfated glycosaminoglycan quantification

Cell viability was assessed via LIVE/DEAD staining per manufacturer instructions (L3224, ThermoFisher Scientific). The amount of sGAG within the cultured beads was assessed via the dimethylmethylene blue (DMMB) assay. For DMMB, groups of 4–5 beads were placed in 2 ml microcentrifuge tubes with alginate dissolving buffer (55 mM sodium citrate, 30 mM EDTA, and 0.15 M NaCl, adjusted to pH 6.0) at a ratio of 100 μ l/bead. Dissolved beads were centrifuged at 500g for 5 min and the supernatant was separated from the remaining cell pellet. DMMB was performed on both the supernatant and the cell pellet separately. We interpreted DMMB results from the supernatant as sGAG dispersed throughout the bead, which we hereafter refer to as the extracellular sGAG. Meanwhile, the cell-associated sGAG within the pellet we refer to as pericellular sGAG. Pellets were digested at 50 °C for at least 1 h with 125 μ l papain digestion solution (125 μ g/ml papain, 0.1 M sodium phosphate monobasic monohydrate, 5 mM EDTA disodium dihydrate, and 5 mM cysteine hydrochloride at pH 6.5). To account for the presence of alginate in samples, a modified DMMB assay was used.²⁹ Briefly, DMMB dye solution was adjusted to a pH of 1.5 and sample absorbances were measured at excitation wavelengths of 525 and 595 nm. The difference between absorbance values at each excitation wavelength was used to determine sGAG concentration in each sample, as compared against a standard curve. For supernatant samples, the standard was chondroitin sulfate (CS) dissolved in alginate dissolving solution, while for pellet samples CS was dissolved in $1\times$ PBS. DNA content was measured using a DNA Quantification Kit (DNAQF, Sigma-Aldrich), and the pericellular and extracellular sGAG measurements were subsequently normalized to DNA content.

2.5 | Immunofluorescence and Immunohistochemistry

To quantify the degree of HSPG degradation from the dose response study, immunofluorescence staining was conducted for the 3G10

neo-epitope created by the enzymatic cleavage of heparan sulfate by heparinase III. Immunohistochemistry (IHC) was also conducted on beads from the osmotic loading study to quantify Heparan sulfate 6-O-Sulftransferase 1 (HS6ST1) enzymatic activity and compare the degree of 6-O sulfation between groups. For both staining techniques, beads were fixed in 10% neutral buffered formalin, embedded in paraffin and 6 μm thick sections taken. Sections were deparaffinized and rehydrated, then blocked, and incubated at 4°C overnight with their respective primary antibody: mouse anti-3G10 heparan sulfate delta primary antibody (H1890-75; US Biological; Salem, MA) at a dilution of 1:100 or a rabbit anti-HS6ST1 primary antibody (ab69682; Abcam, Cambridge, MA) at a dilution of 1:100. The following day the secondary antibodies were applied: goat anti-mouse (ab150113 Alexa Fluor 488; Abcam, Cambridge, MA) at a dilution of 1:100 applied for 1 h or a goat anti-rabbit IgG at 1:100 for 35 min. After secondary staining the sections were rinsed, and counterstained with Hoechst 33258 (1 mg/ml) or Gills Hematoxylin No. 2 and coverslipped. For both techniques, negative controls with omission of the primary antibody were also included.

Images were taken using a Nikon TiE Inverted Microscope at 20x magnification with blinding to the relative groups. Fluorescent images were analyzed for changes in signal intensity using NIS Elements. Briefly, at each heparinase III concentration, intensity profiles for 3G10 and Hoescht channels were captured for individual cell-PCM regions. The peak fluorescent intensity for 3G10 (FITC) channel was normalized to the non-overlapping peak fluorescent intensity for Hoescht (DAPI) channel. 3G10/Hoescht values were then normalized to untreated control.

2.6 | Statistics

Differences in 3G10 stain intensity were assessed via paired *t*-test. Meanwhile, changes in viability after heparinase treatment were assessed via 2-sample *t*-test. Finally, multivariable linear models were used to estimate the association of heparinase III treatment type (untreated and heparinase), osmotic loading (−200, Static, and +200), and time point (1, 2, and 4 weeks) with the outcome measurements of PCM or ECM sGAG/DNA ($\mu\text{g}/\mu\text{g}$). Global *F*-tests for the effect of each factor were conducted and Tukey's multiplicity adjusted pairwise contrasts between levels within each factor were summarized. Each bead within each condition were treated as independent experimental replicates. Analyses were performed using R (version 4.1.2)³⁰ and Minitab. Statistical significance was defined by $p \leq 0.05$.

3 | RESULTS

3.1 | Degradation of HSPGs using heparinase III

Pericellular sGAG/DNA decreased in a dose-dependent manner up to 0.1 U/ml, beyond which there was no discernible change (Figure 1A, C). Degradation was further confirmed via immunofluorescent

staining for the 3G10 neo-epitope created by heparinase III enzymatic cleavage (HS neo-epitope 3G10). 3G10 stain intensity in cell-PCM regions was approximately 1.7 times greater for alginate beads treated with 0.1 U/ml heparinase III compared with untreated control (Figure 1B,C, $p = 0.001$). Importantly, heparinase treatment caused no change in viability ($p = 0.737$; data not shown).

3.2 | Osmotic loading study

Table 1 provides a summary of the global effects (i.e., heparinase treatment, osmotic loading, and time in culture) had on the amount of extracellular and pericellular sGAG/DNA content. Overall there was a significant effect of culture duration ($p < 0.001$) on sGAG/DNA in both ECM and PCM regions, with increasing amounts for longer culture durations (Table 1). The effects of osmotic loading and heparinase treatment are described below. Viability of all groups assessed at 4 weeks was >95% and shown in Figure S3. Mean pericellular and extracellular sGAG/DNA content for each condition are shown in Table S1A and S1B.

3.3 | Effect of osmotic loading on sGAG production

There was a significant effect of osmotic loading on sGAG/DNA content in both extracellular ($p = 0.037$) and pericellular ($p < 0.001$) regions (Figure 2 and Table 1). Extracellular and pericellular sGAG/DNA content generally increased from a hypo-osmotic change (400 \rightarrow 200 mOsm/kgH₂O) to a hyper-osmotic osmotic (400 \rightarrow 600 mOsm/kgH₂O), Figure 2. DNA content is shown in Figure S2 and Table S2. At the pericellular level there were significant differences in sGAG/DNA content between all osmotic groups. Specifically, sGAG/DNA content was lowest in the hypo-osmotic group and highest in the hyper-osmotic group. Both groups were significantly different from the static control. The same directions of effect were observed between the three groups at the extracellular level. However, only the hypo- and hyper-osmotic groups were significantly different, and neither group was significantly different from the static control.

3.4 | Effect of enzyme treatment on sGAG production

There was a significant effect of heparinase III treatment on sGAG/DNA content in the extracellular region ($p < 0.001$; Figure 3 and Table 1). However, there was no significant difference in the pericellular region ($p = 0.51$). Compared with untreated beads, those treated with heparinase III had significantly lower sGAG/DNA content, with an estimated effect size of $-7.3 \mu\text{g sGAG}/\mu\text{g DNA}$. At the pericellular level, there were no significant differences in sGAG/DNA content between the heparinase III and untreated groups. This

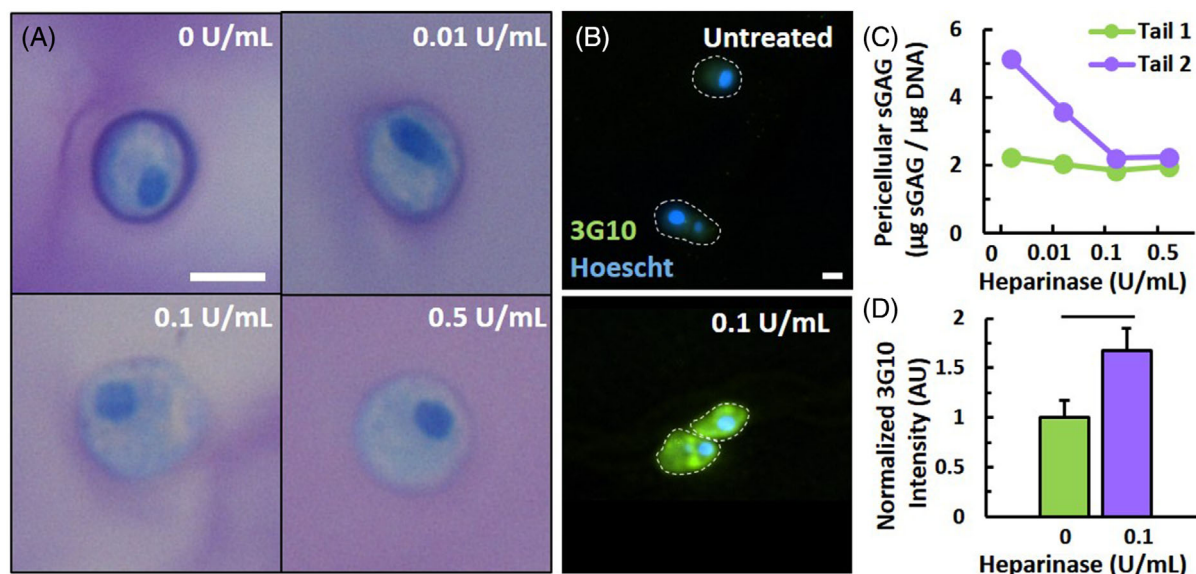


FIGURE 1 Degradation of pericellular sGAG by heparinase III: (A) Toluidine Blue staining demonstrating a reduction in pericellular staining with increased heparinase III concentration. (B) 3G10 heparinase III neo-epitope and Hoescht stain for untreated and 0.1 U/ml heparinase treated cells. (C) Pericellular sGAG measured via modified DMMB assay after 4 h degradation with heparinase III. (D) Quantification of 3G10 stain intensity normalized to Hoescht and untreated cells. Bar denotes a significant difference. Scale bars: 10 µm.

TABLE 1 Summary of effects for sGAG/DNA content

Effect	F test <i>p</i> value		Contrast	ECM sGAG/DNA (µg/µg)		PCM sGAG/DNA (µg/µg)	
	ECM	PCM		Estimate (95% CI)	<i>p</i> value	Estimate (95% CI)	<i>p</i> value
Heparinase treatment	<0.001	0.51	Heparinase vs. untreated	-7.3 (-10.2, -4.4)	<0.001	-0.2 (-0.7, 0.4)	0.51
Osmotic loading	0.037	<0.001	Hypo vs. static	-2.4 (-6.7, 1.8)	0.37	-0.9 (-1.7, -0.1)	0.02
			Hyper vs. static	2.3 (-2, 6.5)	0.42	0.8 (0.04, 1.6)	0.037
			Hyper vs. hypo	4.7 (0.4, 9.0)	0.028	1.7 (0.9, 2.5)	<0.001
Time	<0.001	<0.001	2 vs. 1 weeks	15.7 (11.6, 19.7)	<0.001	1.5 (0.7, 2.2)	<0.001
			4 vs. 1 weeks	42.3 (37.7, 46.9)	<0.001	5.9 (5.1, 6.8)	<0.001
			4 vs. 2 weeks	26.6 (22.2, 31.1)	<0.001	4.5 (3.7, 5.3)	<0.001

Note: Contrasts show per-effect multiplicity-adjusted *p* values and simultaneous confidence intervals.

Note: Bold indicates *p* < 0.05.

suggests that recovery from initial HSPG degradation occurred within the first week of culture.

3.5 | Heparan sulfate 6-O-sulftransferase 1 immunohistochemistry

Pericellular sGAG levels were not different after 1 week of culture. Therefore, HS6ST1 expression was measured to determine whether differences in HSPG sulfation patterns contributed to the observed differences in biosynthesis. Heparan sulfate plays an important role in regulating many cellular functions, through interactions with growth factors, including FGF2. Moreover, changes in HSPG sulfation patterns, particularly at the 6-O residue, are associated with osteoarthritis and other diseases.³¹⁻³⁵ The HS6ST1 enzyme regulates sulfation at the 6-O residue and is upregulated in osteoarthritis. However,

interestingly, results demonstrated HS6ST1 expression in the pericellular region of both heparinase III and untreated controls at all timepoints (Figure 4). This result suggests that the protocol used to isolate cells with their surrounding PCM may have disrupted sulfation patterns. At 1 and 2 weeks, HS6ST1 expression was consistent across samples. Meanwhile, at 4 weeks, HS6ST1 expression was lower in the untreated control groups, independent of osmotic loading condition. This reduction in HS6ST1 staining in the control group may be attributed to recovery from enzymatic cell isolation, while heparinase-treated groups experienced a more delayed recovery.

4 | DISCUSSION

The osmotic environment of the IVD is an important regulator of cellular metabolism, and daily cycles in intra-tissue osmolarity constitute

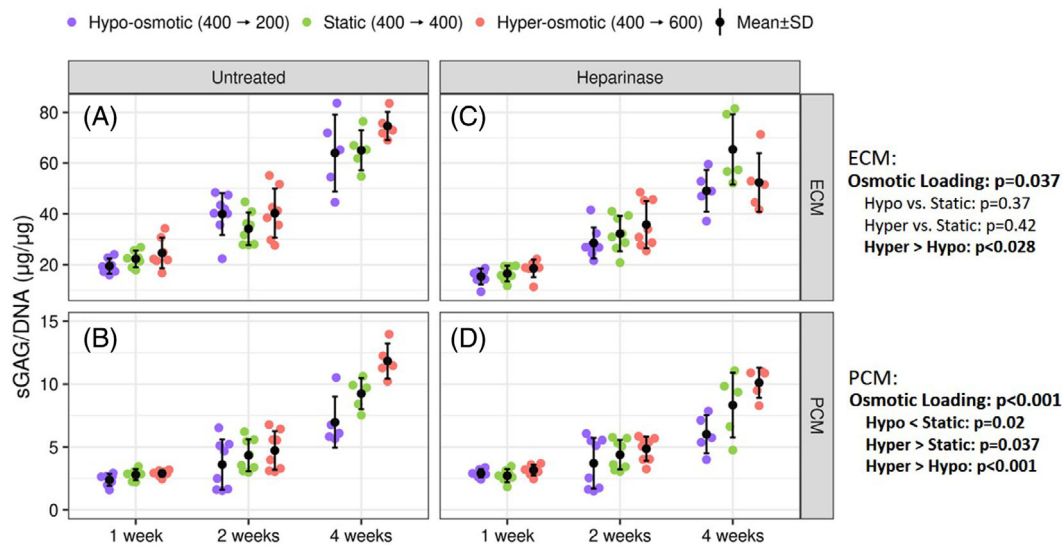


FIGURE 2 Effect of osmotic loading on sGAG synthesis: sGAG/DNA accumulation is shown for beads that were cultured in static osmotic conditions (400→400) or experienced a daily hypo-osmotic (400→200) or hyper-osmotic (400→600) change for 1, 2, or 4 weeks. Beads were either left intact (untreated) (A,B) or treated with heparinase III (C,D) prior to culture. The amount of sGAG/DNA is broken down into the extracellular (A, C) and pericellular (B, D) regions for each osmotic loading condition. The global effect of osmotic loading on sGAG/DNA content was significant for both ECM ($p = 0.037$) and PCM ($p < 0.001$). Averaged across time and treatment, each pairwise difference between osmotic loading levels in the PCM were significant while the ECM showed significant differences only between the hypo- and hyper-osmotic groups.

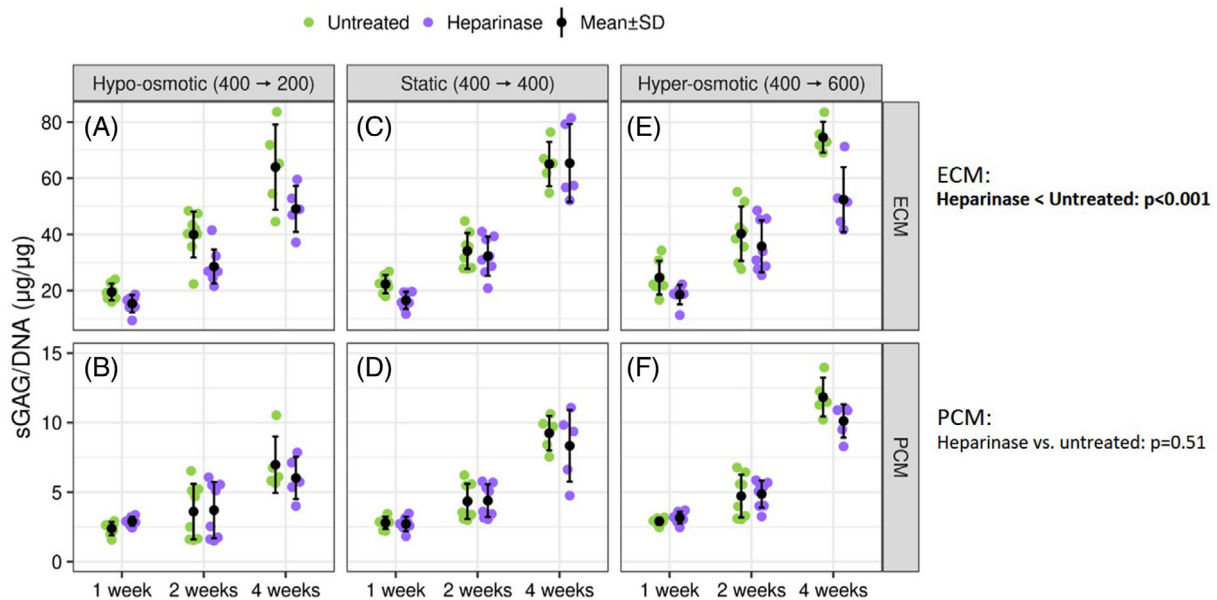


FIGURE 3 Effect of heparinase treatment on sGAG synthesis: sGAG/DNA accumulation is shown for beads that were treated with or without Heparinase III in each osmotic condition. Beads were cultured in static osmotic conditions (C,D) or experienced a daily hypo-osmotic (A,B) or hyper-osmotic (E,F) change for 1, 2, or 4 weeks. The amount of total sGAG/DNA is broken down into the extracellular (A,C,E) and pericellular (B,D,F) regions for each osmotic loading condition. Averaged across time and osmotic condition, mean sGAG/DNA was found to be significantly lower in heparinase treated ECM beads, however, no significant difference by heparinase treatment was observed in the PCM.

a mechanism of mechanotransduction within the IVD.^{1,4,5,7} Although many studies have demonstrated that osmolality influences IVD biology and that cyclic changes in osmolality stimulate metabolism in chondrocytes,⁶ it is unknown whether a cyclic osmotic environment is similarly important for regulating IVD metabolism. Additionally, while

the PCM has been identified as a transducer for the biophysical signals cells experience, whether the region directly mediates the biosynthetic response to cyclic osmotic loading has yet to be determined. Here, we tested the hypotheses: (1) that dynamic osmotic conditions enhance proteoglycan synthesis and (2) that HSPGs within the PCM

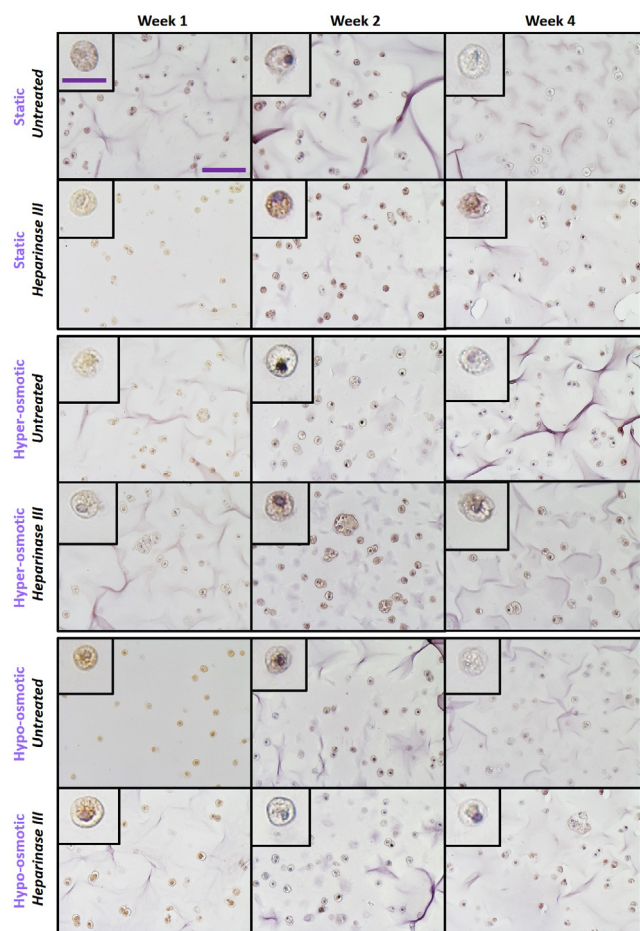


FIGURE 4 HS6ST1 Staining: Representative images of immunohistochemistry staining for the heparan sulfate 6-O-sulfotransferase (HS6ST1) enzyme. Each row represents one experimental condition (e.g., cells treated with or without heparinase III enzyme and cultured in one of the three osmotic culture conditions (hypo-, hyper-, or static). Each column represents a different timepoint of 1, 2, or 4 weeks in culture. Scale bar: 100µm. Inserts: 25µm

alter the biosynthetic response to osmotic loading. Results demonstrate that dynamic osmotic loading did significantly influence cellular metabolism. In particular, a hyper-osmotic change, which represents the osmotic change that would result in-vivo with IVD compression, significantly increased the pericellular sGAG content compared with the static control. Results also demonstrated that initial degradation of pericellular HSPGs resulted in a reduction of extracellular sGAG production, which did not recover even after 4 weeks. This suggests that the composition of the PCM contributes to the metabolic response to osmotic loading. Altogether, this study further demonstrates that the dynamic osmotic environment characteristic to the IVD constitutes a mechanobiologic mechanism, and pericellular HSPGs modulate the metabolic response to osmotic loading.

The first aim of this study was to determine whether a cyclic osmotic environment, simulated by a brief 1 h change in extracellular osmolality, stimulates the biosynthesis of sGAG from NP cells. Overall,

results show that cyclic osmotic loading significantly influenced sGAG production with hyper-osmotic loading increasing sGAG content and hypo-osmotic loading decreasing sGAG content. Additionally, within each region (i.e., PCM and ECM) the effect of hyper- and hypo-osmotic loading on sGAG content was approximately the same magnitude but in opposite directions (Table 1). Cyclic osmotic loading had the largest effect on sGAG content at the pericellular level with significant differences in pericellular sGAG between all three (i.e., static, hypo-, and hyper-osmotically loaded) groups. Specifically, hyper-osmotic loading increased pericellular sGAG by $\sim 0.8 \mu\text{gGAG}/\mu\text{gDNA}$ and hypo-osmotic loading decreased pericellular sGAG by $\sim 0.9 \mu\text{gGAG}/\mu\text{gDNA}$ compared with the static control. Scaling these effect sizes to the collective average of sGAG/DNA within the PCM across all culture durations and conditions demonstrates that osmotic loading modified the amount of sGAG by roughly 18% in both directions relative to static control. Cyclic osmotic loading also influenced extracellular sGAG content, with hyper-osmotic loading inducing significantly more extracellular sGAG accumulation than hypo-osmotic loading, without differing from the static control. However, the effect was less pronounced within the ECM compared with the PCM as hyper- and hypo-osmotic loading increased and decreased the amount of extracellular sGAG accumulation by only $\sim 6\%$ compared the collective average of ECM sGAG, respectively. The finding that there was a more pronounced effect on sGAG content within the pericellular region than extracellular region may be expected, given the relatively short culture duration and the proximity of the PCM to the cell. Still, results demonstrate that cyclic osmotic loading influenced sGAG production in both ECM and PCM regions.

The finding that a hyper-osmotic fluctuation increased sGAG synthesis compared with static conditions is consistent with findings from articular chondrocytes that used a similar loading regimen.⁶ The results further align with the understanding that a hyper-osmotic change mimics the in vivo osmotic environment resulting from tissue compression. Interestingly, a hyper-osmotic change was further shown to mediate the circadian cycle in IVD cells, which highlights the extent to which a cyclic osmotic environment may influence cellular biology.³⁶ However, our results do contrast with findings from a porcine organ culture model, which demonstrated that a simulated diurnal osmotic cycle (430 mOsm/kgH₂O for 8 h and 550 mOsm/kgH₂O for 16 h)³⁷ reduced sGAG accumulation compared to a static 430 mOsm/kgH₂O. Part of the discrepancy may be explained by the different species tested, the scale at which the osmotic conditions were applied (i.e., organ culture vs. cells), and the method through which the solutions were osmotically adjusted (i.e., NaCl vs. sucrose). Specifically, the established dependence of swelling pressure on ionic strength of bathing solutions would suggest that using NaCl to adjust osmotic solutions on whole IVDs may complicate how the ionic/osmotic environment the cells experience within the tissue compares to physiologic.^{2,38} However, despite this difference our results with literature emphasize that a cyclic osmotic environment is an important regulator of sGAG synthesis in NP cells.

The second aim of this study was to determine whether pericellular HSPGs influenced the biosynthetic response to osmotic

loading. Overall, degradation of HSPGs with heparinase-III significantly decreased extracellular sGAG accumulation. However, while osmotic loading had a similar effect at both the peri- and extra-cellular levels, heparinase treatment only significantly affected the amount of extracellular sGAG. This finding suggests that during the initial phase of culture, heparinase-treated cells from all loading conditions were preferentially re-establishing their pericellular matrix prior to the broader dispersion of sGAG to the surrounding hydrogel, which is in accordance with previous studies.^{39,40} Interestingly, at 1 week HSPG degradation reduced mean extracellular sGAG content by 21–26% for all osmotic conditions. However, at 4 weeks, the static control exhibited no difference in extracellular sGAG between untreated and heparinase III treated groups. Meanwhile, heparinase-treated cells from both the hypo- and hyper-osmotically loaded groups maintained sGAG deficits at 4 weeks—23% and 29%, respectively. This suggests that static conditions were conducive for cells to restore the biosynthetic function of the PCM, while cyclic conditions hindered that functional repair.

The composition and corresponding mechanical properties of the PCM influence cellular deformations under various chemical and mechanical conditions and alterations in cellular scale deformations is one mechanobiologic mechanism through which the PCM influences cellular metabolism. Specifically under osmotic loading, changes to PCM composition have been shown to influence the degree of cellular swelling and intracellular calcium signal.^{24,41} However, the macro- and micro- mechanical behaviors of orthopedic soft-tissues have long been understood to be influenced by the interplay between the proteoglycans within the tissue and the collagen network in which they are confined.^{21,38,42–44} In particular, pre-stressing or tensioning of the collagen network due to osmotic swelling contributes to the nonlinear compression/tension behaviors of articular cartilage^{38,45,46} and modeling studies have suggested a similar phenomenon occurs at the microscale within the PCM.⁴⁷ Degradation of the HSPGs within the PCM would reduce the local FCD and swelling pressures within the PCM which could presumably influence the degree of pre-stress on the collagen fibers. Additionally, the local osmotic environment can also directly impact the organization of the collagen fibers themselves.⁴⁴ These local changes to the pericellular collagen organization and stress states may alter the effective modulus of the PCM and influence its resistance to deformation under mechanical or chemical conditions. Recent work using a decorin knock-out mouse model demonstrated that the absence of pericellular decorin, another sGAG, decreased the effective modulus of the PCM⁴¹ and similarly found that the absence of pericellular decorin reduced amounts of extracellular GAG expression. Interestingly, a previous study on porcine articular cartilage used atomic force microscopy to investigate how degradation of pericellular HSPGs influenced the elastic modulus of the PCM and similarly used heparinase III. They observed that heparinase III degradation of pericellular HSPG increased the modulus of the PCM compared to untreated cells.²¹ This finding together with our results demonstrating a consistent reduction in extracellular sGAG in heparinase treated cells at 1 week compared to untreated controls suggests that a mechanobiologic consequence of an increased

pericellular modulus may be associated with depressed extracellular sGAG synthesis. Collectively, our results together with the literature suggest that modifications to the sGAG content within the PCM alter the FCD and effective modulus of the PCM and are an important regulator of mechanobiology.

In a variety of tissues, HSPG sulfation pattern is more influential than HSPG quantity. Specifically, distinct patterns of HSPG sulfation are present in healthy and diseased tissues, although HSPG quantity itself is not different.³³ Recent work by Chanalaris et al. identified HSPG dysregulation as a contributor to osteoarthritis, with significant changes to the expression of HSPG core proteins, modifying enzymes, and sulfation patterns present in osteoarthritic tissue.³³ Therefore, here we investigated potential changes in sulfation patterns by examining protein expression of the HS6ST1 enzyme. Interestingly, HS6ST1 expression was consistent across groups at 1 and 2 weeks. This suggests that the initial cell-PCM isolation may have promoted HS6ST1 expression as a PCM repair mechanism. Meanwhile, at week 4, HS6ST1 expression decreased in the untreated control group. Therefore, static conditions may be interpreted as more conducive to PCM repair. However, further work is needed to validate this interpretation. From a mechanical perspective, HSPG regions represent the softest of all tissue matrix,²¹ and the region's stiffness is further reduced with osteoarthritis.⁴⁸ These findings suggest that the HSPG region in particular is uniquely equipped to tolerate cell deformation and cell volume changes. Thus, while regulation of cell volume adaptation by the PCM has been well-studied,^{23,24,49–51} HSPGs in particular likely have an unexplored role in morphology and volume regulation, as well as a yet unseen influence on the broader transduction of mechano-osmotic stimuli. Future studies will be necessary to determine the precise mechanisms responsible for these findings. However, results collectively suggest that heparinase III treatment irreversibly altered critical mechanisms within the PCM (likely both biological and mechanical), responsible for modulating the anabolic response to osmotic fluctuations.

It is necessary to note that there are several limitations to the current study. Importantly, due to the required cell yield for these experiments, a separate cell isolation was required for each time point in order to obtain a sufficient cell number with retained PCM. Therefore, separate populations of cells were used at the separate time points, which impacts the ability to compare directly between culture durations. Nevertheless, the use of five tails for each isolation provides a relatively spread pool for averaging of cellular profiles, and thus enables some degree of assessment between time points. Further, as a result of the sample size we do not have sufficient statistical power to make every pair-wise comparison and our interpretation is limited to pair-wise comparisons within each global factor (i.e., heparinase treatment, osmotic loading, and time). Additionally, the standard used for DMMB measurements of PCM sGAG was chondroitin sulfate, which comprises distinct disaccharide repeats from heparan sulfate, and thus exhibits a different binding mechanism with DMMB dye. This difference in binding would likely alter the precise quantity of PCM sGAG reported by the assay, potentially underestimating the sGAG/DNA content within the PCM region, but the expected trends

would be comparable. Potentially more notable, the low dye pH used in the modified DMMB assay, which was necessitated by interactions between the dye and the alginate itself, has been shown to cause decreased sensitivity for heparan sulfate compared to chondroitin sulfate.²⁹ Therefore, it is possible that the absence of differences due to heparinase treatment in the pericellular region could partially be attributed to the reduced sensitivity of the assay for HSPGs, which are the predominate pericellular sGAG. Lastly, the exact age of the animals from which cells were isolated is unknown. However, tissue was obtained from animals entering the food supply which are generally representative of juvenile animals. Despite these limitations, the primary conclusions of the study were considered reasonable.

In this study, cyclic hyper-osmotic loading significantly increased pericellular sGAG accumulation compared to a static osmotic environment, and degradation of pericellular HSPGs reduced extracellular sGAG synthesis under dynamic osmotic conditions. The sustained suppression of sGAG synthesis under dynamic conditions suggests that changes to HSPG composition in degeneration may directly contribute to the abnormal metabolic responses of cells to mechanical loading. Collectively, these findings prompt closer investigations of mechanotransduction events that originate within the HSPG region and of potential alterations to HSPG-associated signaling during the progression of degeneration. Ultimately, this study further distinguishes heparan sulfate proteoglycans (and their structural heterogeneity) as potential targets for modulating mechanotransduction in disease.

AUTHOR CONTRIBUTIONS

Carly M. Krull, Devina Purmessur, and Benjamin A. Walter were involved in the design of this study. Carly M. Krull, and Jordan Rife collected the data. Carly M. Krull, Jordan Rife, Brett Klamer, Devina Purmessur, and Benjamin A. Walter analyzed and interpreted the data. Carly M. Krull and Benjamin A. Walter wrote the manuscript. All authors have read, revised and approved the final manuscript.

ACKNOWLEDGMENTS

Research reported in this publication was supported by the National Institute of Arthritis and Musculoskeletal and Skin Diseases of the National Institutes of Health under award number R21AR076611, by the National Center for Advancing Translational Sciences of the National Institutes of Health under Grant Number UL1TR002733, and by The Ohio State University Department of Biomedical Engineering. The content is solely the responsibility of the authors and does not necessarily represent the official views of the National Institutes of Health. We would like to acknowledge Jesse Keckler and the Spine Research Institute for assistance designing and manufacturing the transwell inserts and Gillian Gunsch and Shirley Tang for assistance with the immunohistochemistry.

CONFLICT OF INTEREST

The authors declare no conflict of interest.

ORCID

Benjamin A. Walter  <https://orcid.org/0000-0002-0742-5533>

REFERENCES

- Lai WM, Hou JS, Mow VC. A triphasic theory for the swelling and deformation behaviors of articular cartilage. *J Biomech Eng.* 1991;113:245-258.
- Buschmann MD, Grodzinsky AJ. A molecular model of proteoglycan-associated electrostatic forces in cartilage mechanics. *J Biomech Eng.* 1995;117:179-192.
- Zimmerman BK, Nims RJ, Chen A, Hung CT, Ateshian GA. Direct osmotic pressure measurements in articular cartilage demonstrate nonideal and concentration-dependent phenomena. *J Biomech Eng.* 2021;143:041007.
- Urban JP, Maroudas A, Bayliss MT, Dillon J. Swelling pressures of proteoglycans at the concentrations found in cartilaginous tissues. *Biorheology.* 1979;16:447-464.
- Ishihara H, Warensjo K, Roberts S, Urban JP. Proteoglycan synthesis in the intervertebral disk nucleus: the role of extracellular osmolality. *Am J Physiol.* 1997;272:C1499-C1506.
- O'Connor CJ, Leddy HA, Benefield HC, Liedtke WB, Guilak F. TRPV4-mediated mechanotransduction regulates the metabolic response of chondrocytes to dynamic loading. *Proc Natl Acad Sci USA.* 2014;111:1316-1321.
- Sivan S, Neidlinger-Wilke C, Wurtz K, Maroudas A, Urban JP. Diurnal fluid expression and activity of intervertebral disc cells. *Biorheology.* 2006;43:283-291.
- Botsford DJ, Esses SI, Ogilvie-Harris DJ. In vivo diurnal variation in intervertebral disc volume and morphology. *Spine (Phila Pa 1976).* 1994;19:935-940.
- Chan SC, Ferguson SJ, Gantenbein-Ritter B. The effects of dynamic loading on the intervertebral disc. *Eur Spine J.* 2011;20:1796-1812.
- Fearing BV, Hernandez PA, Setton LA, Chahine NO. Mechanotransduction and cell biomechanics of the intervertebral disc. *JOR Spine.* 2018;1:e1026.
- Boyd LM, Richardson WJ, Chen J, Kraus VB, Tewari A, Setton LA. Osmolarity regulates gene expression in intervertebral disc cells determined by gene array and real-time quantitative RT-PCR. *Ann Biomed Eng.* 2005;33:1071-1077.
- Wuertz K, Urban JP, Klases J, et al. Influence of extracellular osmolality and mechanical stimulation on gene expression of intervertebral disc cells. *J Orthop Res.* 2007;25:1513-1522.
- Krouwels A, Popov-Celeketi J, Plomp SGM, et al. No effects of hyperosmolar culture medium on tissue regeneration by human degenerated nucleus Pulposus cells despite upregulation extracellular matrix genes. *Spine (Phila Pa 1976).* 2018;43:307-315.
- Walter BA, Purmessur D, Moon A, et al. Reduced tissue osmolality increases TRPV4 expression and pro-inflammatory cytokines in intervertebral disc cells. *Eur Cell Mater.* 2016;32:123-136.
- Chao PH, West AC, Hung CT. Chondrocyte intracellular calcium, cytoskeletal organization, and gene expression responses to dynamic osmotic loading. *Am J Physiol Cell Physiol.* 2006;291:C718-C725.
- O'Connell GD, Newman IB, Carapezza MA. Effect of long-term osmotic loading culture on matrix synthesis from intervertebral disc cells. *Biores Open Access.* 2014;3:242-249.
- Krouwels A, Melchels FPW, van Rijen MHP, et al. Comparing hydrogels for human nucleus pulposus regeneration: role of osmolality during expansion. *Tissue Eng Part C Methods.* 2018;24:222-232.
- Hayes AJ, Melrose J. 3D distribution of perlecan within intervertebral disc chondrons suggests novel regulatory roles for this multifunctional modular heparan sulphate proteoglycan. *Eur Cell Mater.* 2021;41:73-89.
- Guilak F, Nims RJ, Dicks A, Wu CL, Meulenbelt I. Osteoarthritis as a disease of the cartilage pericellular matrix. *Matrix Biol.* 2018;71-72:40-50.
- Guilak F, Alexopoulos LG, Upton ML, et al. The pericellular matrix as a transducer of biomechanical and biochemical signals in articular cartilage. *Ann N Y Acad Sci.* 2006;1068:498-512.

21. Wilusz RE, Sanchez-Adams J, Guilak F. The structure and function of the pericellular matrix of articular cartilage. *Matrix Biol.* 2014;39:25-32.
22. Hayes AJ, Shu CC, Lord MS, Little CB, Whitelock JM, Melrose J. Pericellular colocalisation and interactive properties of type VI collagen and perlecan in the intervertebral disc. *Eur Cell Mater.* 2016;32:40-57.
23. Haider MA, Schugart RC, Setton LA, Guilak F. A mechano-chemical model for the passive swelling response of an isolated chondron under osmotic loading. *Biomech Model Mechanobiol.* 2006;5:160-171.
24. Zelenski NA, Leddy HA, Sanchez-Adams J, et al. Type VI collagen regulates pericellular matrix properties, chondrocyte swelling, and mechanotransduction in mouse articular cartilage. *Arthritis Rheumatol.* 2015;67:1286-1294.
25. Lamanna WC, Kalus I, Padva M, Baldwin RJ, Merry CL, Dierks T. The heparanome: the enigma of encoding and decoding heparan sulfate sulfation. *J Biotechnol.* 2007;129:290-307.
26. Lee GM, Poole CA, Kelley SS, Chang J, Caterson B. Isolated chondrons: a viable alternative for studies of chondrocyte metabolism in vitro. *Osteoarthr Cartil.* 1997;5:261-274.
27. Vedicherla S, Buckley CT. Rapid chondrocyte isolation for tissue engineering applications: the effect of enzyme concentration and temporal exposure on the matrix forming capacity of nasal derived chondrocytes. *Biomed Res Int.* 2017;2017:2395138.
28. Walter BA, Torre OM, Laudier D, Naidich TP, Hecht AC, Iatridis JC. Form and function of the intervertebral disc in health and disease: a morphological and stain comparison study. *J Anat.* 2015;227:707-716.
29. Zheng CH, Levenston ME. Fact versus artifact: avoiding erroneous estimates of sulfated glycosaminoglycan content using the dimethylmethylene blue colorimetric assay for tissue-engineered constructs. *Eur Cell Mater.* 2015;29:224-236. discussion 36.
30. *R: A Language and Environment for Statistical Computing.* R Foundation for Statistical Computing; 2021.
31. Alhasan AA, Spielhofer J, Kusche-Gullberg M, Kirby JA, Ali S. Role of 6-O-sulfated heparan sulfate in chronic renal fibrosis. *J Biol Chem.* 2014;289:20295-20306.
32. Shamdani S, Chantepie S, Flageolet C, et al. Heparan sulfate functions are altered in the osteoarthritic cartilage. *Arthritis Res Ther.* 2020;22:283.
33. Chanalaris A, Clarke H, Guimond SE, Vincent TL, Turnbull JE, Troeberg L. Heparan sulfate proteoglycan synthesis is dysregulated in human osteoarthritic cartilage. *Am J Pathol.* 2019;189:632-647.
34. Severmann AC, Jochmann K, Feller K, et al. An altered heparan sulfate structure in the articular cartilage protects against osteoarthritis. *Osteoarthr Cartil.* 2020;28:977-987.
35. Soares da Costa D, Reis RL, Pashkuleva I. Sulfation of glycosaminoglycans and its implications in human health and disorders. *Annu Rev Biomed Eng.* 2017;19:1-26.
36. Dudek M, Pathirana D, Goncalves C, et al. Mechanical loading and hyperosmolarity as a daily resetting cue for skeletal circadian clocks. *bioRxiv.* 2021.
37. Li P, Gan Y, Xu Y, et al. Osmolarity affects matrix synthesis in the nucleus pulposus associated with the involvement of MAPK pathways: a study of ex vivo disc organ culture system. *J Orthop Res.* 2016;34:1092-1100.
38. Canal Guterl C, Hung CT, Ateshian GA. Electrostatic and non-electrostatic contributions of proteoglycans to the compressive equilibrium modulus of bovine articular cartilage. *J Biomech.* 2010;43:1343-1350.
39. Kuettner KE, Pauli BU, Gall G, Memoli VA, Schenk RK. Synthesis of cartilage matrix by mammalian chondrocytes in vitro. I. Isolation, culture characteristics, and morphology. *J Cell Biol.* 1982;93:743-750.
40. McLeod CM, Mauck RL. High fidelity visualization of cell-to-cell variation and temporal dynamics in nascent extracellular matrix formation. *Sci Rep.* 2016;6:38852.
41. Chery DR, Han B, Zhou Y, et al. Decorin regulates cartilage pericellular matrix micromechanobiology. *Matrix Biol.* 2021;96:1-17.
42. Han B, Nia HT, Wang C, et al. AFM-nanomechanical test: an interdisciplinary tool that links the understanding of cartilage and meniscus biomechanics, osteoarthritis degeneration, and tissue engineering. *ACS Biomater Sci Eng.* 2017;3:2033-2049.
43. Chahine NO, Chen FH, Hung CT, Ateshian GA. Direct measurement of osmotic pressure of glycosaminoglycan solutions by membrane osmometry at room temperature. *Biophys J.* 2005;89:1543-1550.
44. Han WM, Nerurkar NL, Smith LJ, Jacobs NT, Mauck RL, Elliott DM. Multi-scale structural and tensile mechanical response of annulus fibrosus to osmotic loading. *Ann Biomed Eng.* 2012;40:1610-1621.
45. Ateshian GA, Soltz MA, Mauck RL, Basalo IM, Hung CT, Lai WM. The role of osmotic pressure and tension-compression nonlinearity in the frictional response of articular cartilage. *Transp Porous Media.* 2003;50:5-33.
46. Chahine NO, Wang CC, Hung CT, Ateshian GA. Anisotropic strain-dependent material properties of bovine articular cartilage in the transitional range from tension to compression. *J Biomech.* 2004;37:1251-1261.
47. Likhithpanichkul M, Guo XE, Mow VC. The effect of matrix tension-compression nonlinearity and fixed negative charges on chondrocyte responses in cartilage. *Mol Cell Biomech.* 2005;2:191-204.
48. Alexopoulos LG, Haider MA, Vail TP, Guilak F. Alterations in the mechanical properties of the human chondrocyte pericellular matrix with osteoarthritis. *J Biomech Eng.* 2003;125:323-333.
49. Hing WA, Sherwin AF, Poole CA. The influence of the pericellular microenvironment on the chondrocyte response to osmotic challenge. *Osteoarthr Cartil.* 2002;10:297-307.
50. Choi JB, Youn I, Cao L, et al. Zonal changes in the three-dimensional morphology of the chondron under compression: the relationship among cellular, pericellular, and extracellular deformation in articular cartilage. *J Biomech.* 2007;40:2596-2603.
51. Tanska P, Turunen SM, Han SK, Julkunen P, Herzog W, Korhonen RK. Superficial collagen fibril modulus and pericellular fixed charge density modulate chondrocyte volumetric behaviour in early osteoarthritis. *Comput Math Methods Med.* 2013;2013:164146.

SUPPORTING INFORMATION

Additional supporting information may be found in the online version of the article at the publisher's website.

How to cite this article: Krull, C. M., Rife, J., Klammer, B., Purmessur, D., & Walter, B. A. (2022). Pericellular heparan sulfate proteoglycans: Role in regulating the biosynthetic response of nucleus pulposus cells to osmotic loading. *JOR Spine*, 5(2), e1209. <https://doi.org/10.1002/jsp2.1209>